

## Review

# Pressure monitoring on the real thin inter-layer gas reservoir by time-lapse seismic method

Jingye Li<sup>1\*</sup> Wang Shoudong<sup>2</sup>

<sup>1</sup> Department of Geophysics, China University of Petroleum, Beijing, China.

<sup>2</sup> Department of Geophysics, China University of Petroleum, Beijing, China.

Accepted 11 September, 2011.

The effective pressure monitoring is very important to the management of the gas reservoir. In this paper, we presented a case of pressure monitoring in the thin inter-layer gas reservoir by time-lapse seismic method. During this study, the novel time-lapse seismic difference impedance inversion method was presented based on pre-stack elastic impedance inversion theory. The computational experiments show that the relationships constructed on the log data and the core lab data can not be used to compute the thin inter-layer reservoir parameters variations from the P wave and S wave impedance and their differences, such as pressure and saturation. The reason is that the measurement scale differences between seismic data and log data make the relationships inconsistent. Therefore, the accumulative attributes are tested, verified, and then applied for pressure variation prediction on the inversed impedance differences. The computed results have good conformance with the matters of fact of the real gas reservoir.

**Keywords:** Time-lapse, pressure monitor, gas reservoir, accumulative attribute, difference inversion.

## INTRODUCTION

Time-lapse seismic reservoir monitoring technology, as one of the most important development seismic methods, is very useful in search of residual oil and improvement of the managements of oil and gas reservoirs (Brown et al., 2007). During the development of the gas reservoir, the water saturation can be changed by fluid substitution from gas to water. At the same time, the effective pressure can also be changed when the injected

water is not enough or even no water is supplied. The decrease of the fluid pressure can cause the effective pressure loaded on the rock increase. The micro-crack will be closed and then the permeability will decrease when the effective pressure loaded on the rock is higher. So pressure monitoring is very important to the management of the gas reservoir (Davis and Benson, 2008). But in the past time-lapse seismic study, more attention was put on the saturation variation, and little

attention on pressure variation. The reason is that the coupled time-lapse seismic responses caused by saturation and pressure variations are hard to be separated by the post-stack time-lapse seismic data. In recent years, the analysis on core lab data and field data shows that there are different variations rules for P wave, S wave velocities and density varying with saturation and pressure. So it is feasible to predict the pressure and saturation variations from time-lapse seismic pre-stack data differences. And then many studies have been conducted on time-lapse AVO simulation, pre-stack AVO inversion and time-lapse seismic application (Ying and Laurance, 2003; Landro, 2003). However, for the thin inter-layer gas reservoir, we encounter the new challenges of how to improve the precision of time-lapse difference impedance and how to interpret the seismic-scale difference impedance (Zeng, 2009; Maffilietti et al., 2010; Grey et al., 2000). In this paper, we present a pressure monitoring case in a real thin inter-layer gas reservoir by time-lapse seismic method. During the study, the novel time-lapse seismic difference impedance inversion method and the

\*Corresponding author email: [lijingye1@gmail.com](mailto:lijingye1@gmail.com)

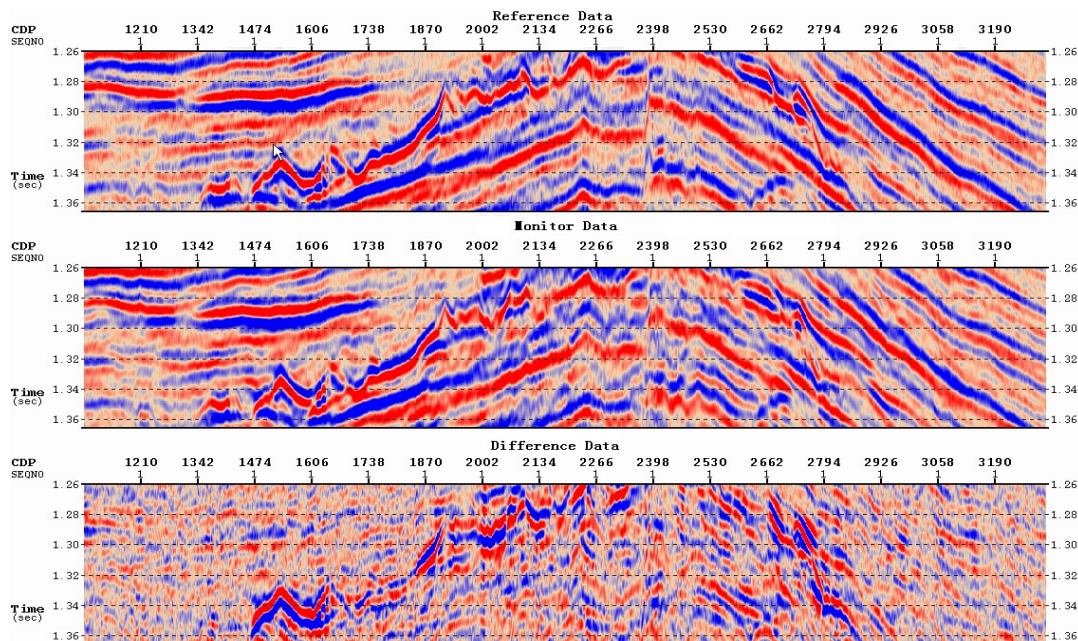


**Figure 1.** The reference seismic data (top), the monitor seismic data (middle) and their difference (bottom) of the time-lapse near-offset seismic data after matching process

accumulative attributes are presented and applied. The results have good conformance with the matters of fact in the real gas reservoir.

### Background of the real gas reservoir

The real case we studied is an offshore gas field. The gas reservoir is a thin shale sand inter-layer formation with strong heterogeneity caused by the mud flow, the waves and the tides. The interpretation of log data show that there are 45 thin sand layers mixed with other shale and sand shale layers. The average porosity of all sand layers is about 25%. The bottom-hole well-bore pressure is decreasing during the gas production. The main reason is that there are no water injection and no enough bottom water supplies. And the decrease of fluid pressure also causes the decrease of production capacity of the gas reservoir. So defining the range of fluid pressure decreasing is valuable for improve the production capacity and optimize the developing scheme. We have acquired one time seismic data before the gas reservoir development and another time after its development. We conducted matching process on the far-offset and the near-offset time-lapse seismic data respectively. The near-offset reference data, monitor data and their difference data after matching process are shown as in Figure1. Based on these data, we compute impedance difference by inversion method

for the pressure dynamic monitoring in the gas reservoir.

### Elastic impedance difference inversion method

Connolly (1999) presented the concept and expression of elastic impedance ( $EI$ ), shown as equation 1:

$$EI = V_p (V_p^{\tan^2 \theta} V_s^{-8K \sin^2 \theta} \rho^{(1-4K \sin^2 \theta)}) \quad (1)$$

Where  $V_p$ ,  $V_s$  and  $\rho$  are P wave velocity, S wave velocities, and density respectively;  $\theta$  is incident angle and  $K = (V_s / V_p)^2$ . Therefore, the elastic impedance, generalized acoustic impedance, is the function of P wave velocity, S wave velocity, and density and incident angle. Similar to AVO inversion, the elastic impedance inversion can be applied to compute the formation elastic parameters, such as P wave impedance and S wave impedance, which are useful for reservoir saturation and pressure monitor.

For the time-lapse seismic, there are two or even more times seismic data. In general, these data can be inverted respectively to obtain the elastic parameters and their differences for reservoir dynamic characterization. But in this paper, to take the time-lapse seismic difference data as a constraint and to reduce the inversion calculation and obtain the elastic parameters differences directly, we applied a novel elastic impedance inversion method directly on the time-lapse

seismic difference data.

The relation of the incident angle  $\theta$ , the elastic impedance  $EI$  and the reflection coefficient  $\gamma$  can be shown as.

$$r(\theta, t_i) = \frac{EI(t_i) - EI(t_{i-1})}{EI(t_i) + EI(t_{i-1})} \quad (2)$$

Under the assumption that the formations under surface are continuous medium, the approximation can be

$$\text{shown as: } 2EI(t_i) \approx EI(t_{i+1}) + EI(t_i) \quad (3)$$

$$EI(t_{i+1}) - EI(t_i) \approx \Delta t \frac{dEI(t_i)}{dt} \quad (4)$$

For seismic data,  $\Delta t$  is a constant, so the reflection coefficient  $\gamma$  is

$$\gamma(t) \approx \frac{1}{2} \frac{d \ln EI(t)}{dt} \quad (5)$$

If  $li_i = \ln EI_i$ , the relationship between the seismic data, the wavelet  $B$  and the elastic impedance can be written as:

$$\begin{pmatrix} s_0 \\ s_1 \\ s_2 \\ s_3 \\ s_4 \\ s_5 \\ s_6 \\ s_7 \\ s_8 \\ s_9 \\ s_{10} \end{pmatrix} = \begin{pmatrix} 0 & & & & & & & & & & & \\ -b_1 & b_1 & & & & & & & & & & \\ -b_2 b_2 - b_1 & b_1 & & & & & & & & & & \\ -b_3 b_3 - b_2 & b_2 - b_1 & b_1 & & & & & & & & & \\ -b_4 b_4 - b_3 & b_3 - b_2 & b_2 - b_1 & b_1 & & & & & & & & \\ -b_5 b_5 - b_4 & b_4 - b_3 & b_3 - b_2 & b_2 - b_1 & b_1 & & & & & & & \\ -b_6 & b_5 - b_4 & b_4 - b_3 & b_3 - b_2 & b_2 - b_1 & b_1 & & & & & & \\ & & & & & & b_2 - b_1 & b_1 & & & & \\ & & & & & & & b_2 - b_1 & b_1 & & & \\ & & & & & & & & & b_2 - b_1 & b_1 & \\ & & & & & & & & & & & -b_3 & b_3 - b_2 & b_2 - b_1 & b_1 \end{pmatrix} \begin{pmatrix} li_0 \\ li_1 \\ li_2 \\ li_3 \\ li_4 \\ li_5 \\ li_6 \\ li_7 \\ li_8 \\ li_9 \\ li_{10} \end{pmatrix} \quad (6)$$

The upper relation can be simplified as  $S = BL$  in matrix form. For the time-lapse seismic, the first time data  $S_1 = BL_1$ , and the second time data  $S_2 = BL_2$ , the relation between time-lapse seismic data difference and the elastic impedance difference can be shown as:

$$\delta S = B\delta L \quad (7)$$

Where,  $\delta S = S_2 - S_1$ , and  $\delta L = L_2 - L_1$ . The relation is

uniform with the relation between seismic data and elastic impedance (Connolly, 1999). To solve equation 7 for time-lapse seismic impedance difference inversion, we defined the objective function as:

$$\| \delta S - B\delta L \| + \alpha \| D\delta L \| + \beta \| M\delta L - M\delta L^* \| \quad (8)$$

Where,  $\delta L^*$  is initial difference model,

and  $\alpha$  and  $\beta$  are weight factors. To minimize the objective function, the equation 9 should be solved.

$$(B^T B + \alpha D^T D + \beta M^T M) \delta L = B^T \delta S + \beta M^T M \delta L^* \quad (9)$$

Where,  $\delta L^*$  is initial impedance difference model, another constraint for time-lapse seismic difference inversion. To construct the initial impedance difference model, we require both the horizon interpreted on seismic data and the log data variation between before and after the development of the gas reservoir. In the real gas field, the log data after the reservoirs development are hard to be measured. So using the information, including the log data measured in the field and its interpretation before development, temperature, pressure and saturation variations measured during production and/or calculated by reservoir simulation, we conduct the log data prediction after the reservoir development for the initial difference impedance model construction (Mavko et al., 2008; Batzle and Wang 1992; Shaprio, 2003; Gassmann, 1951). The workflow we applied for the log data prediction after the reservoir development is shown as in Figure 2.

Next, we compute the P-wave impedance, S-wave impedance and their differences caused by the reservoir development on the reference seismic data and the seismic data difference. The computed results are shown as in Figure 3 and Figure 4.

### Pressure monitoring on inversion difference data

During the gas reservoir development, both the effective pressure and the water saturation can be changed. And both of them can cause the P-wave and S-wave impedance variation. According to the rock physical model and the core lab data for the sandstone reservoir, the water saturation variation mainly causes the change of P-wave velocity, but has little effect on S-wave velocity. And the effective pressure variation can affects

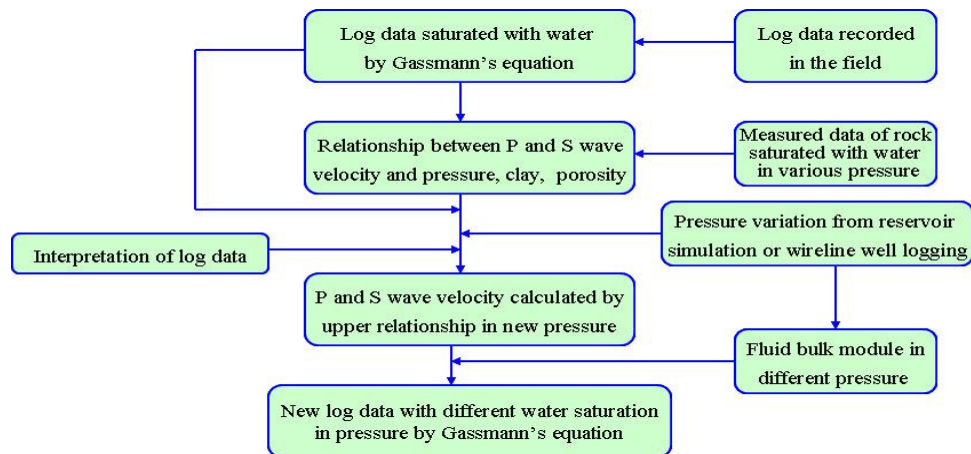


**Figure 2.** The work flow of log data prediction after the gas reservoir development

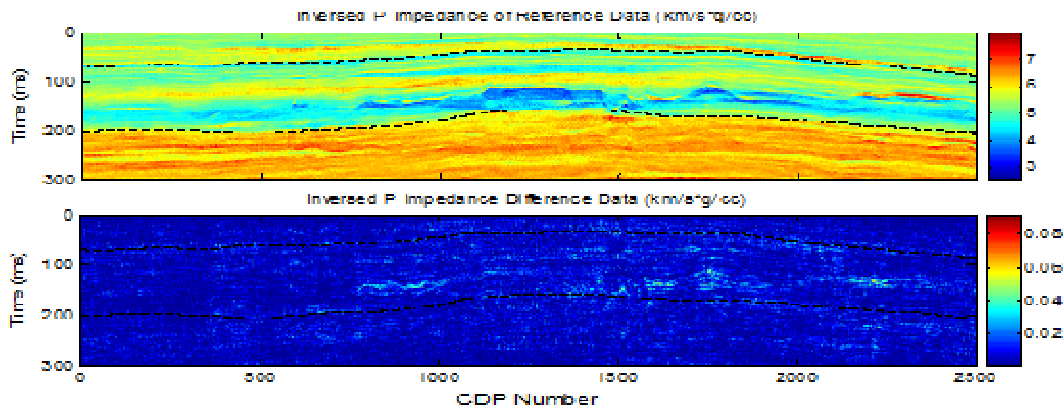


**Figure 3.** The inversed P-wave impedance (top) from the reference data and the inversed P-wave impedance variation (bottom) from the time-lapse seismic difference data. The color-bar is P-wave impedance for the upper figure and their difference for the lower one.

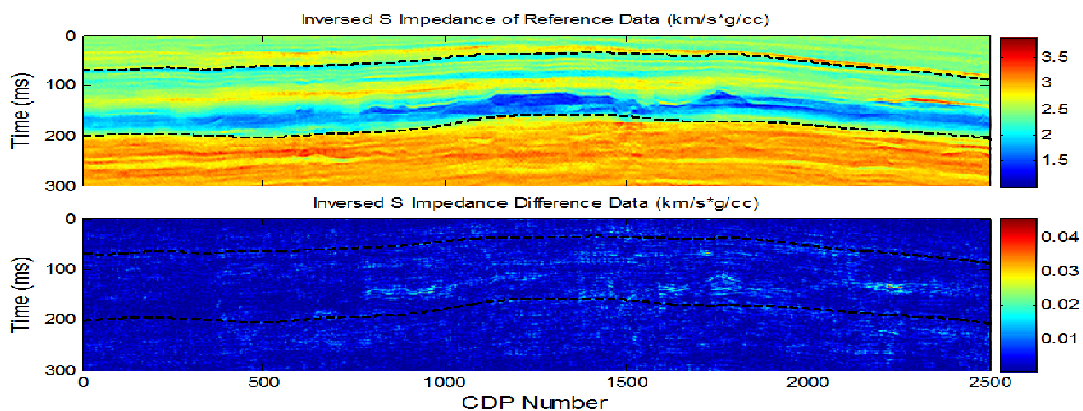


**Figure 4.** The inversed S-wave impedance (top) from the reference data and the inversed S-wave impedance variation (bottom) from the time-lapse seismic difference data. The color-bar is S-wave impedance for the upper figure and their difference for the lower one.

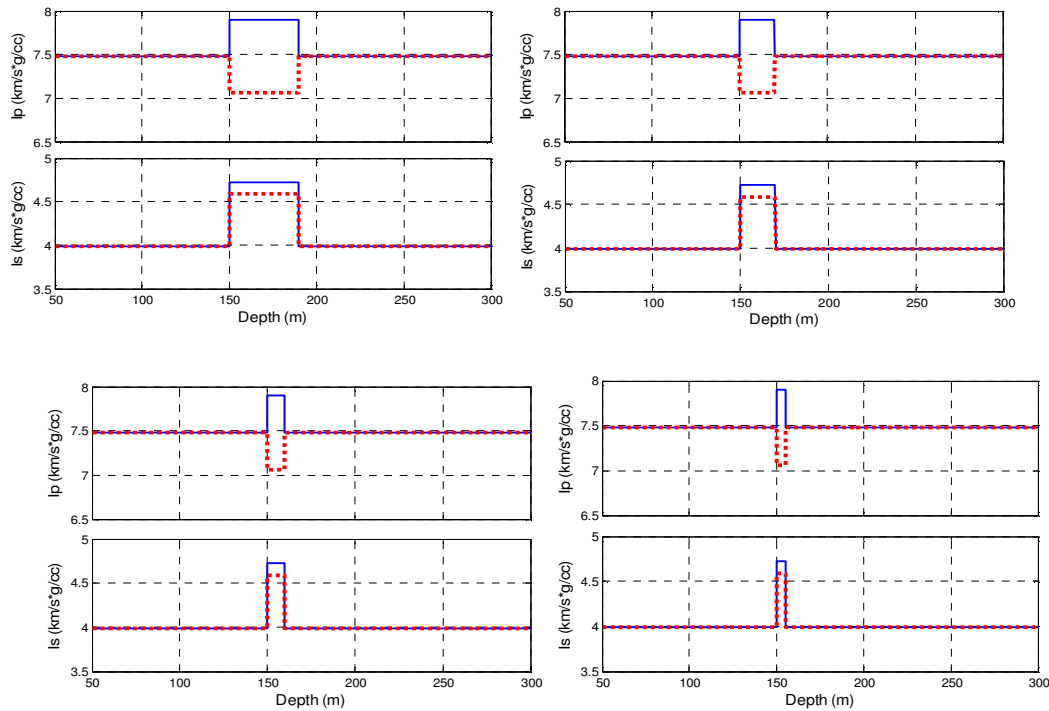


**Figure 5.** The accurate model of P-wave impedance and S-wave impedance with different sand thicknesses, from top to bottom and from left to right: the sand formation thickness is 1/2, 1/4, 1/8, and 1/16 wavelength. The blue solid lines are for wet formations and red dotted lines are for gas formations with water saturation 0.4

both P-wave and S-wave velocities (Gassmann, 1951; Ebhart-Phillips et al., 1989). That is, the P-wave impedance is sensitive to both effective pressure and water saturation. But the S-wave impedance is only sensitive to effective pressure.

For the thick formation, the variations of the reservoir parameters can be computed from the inversed P-wave and S-wave impedance differences directly by the rock physical relations between elastic parameters and reservoir parameters obtained on log data and core lab data. But in the case of the thin inter-layer gas reservoir, we can not use the relationships constructed on the log data and lab data to compute the reservoir parameters variations, such as pressure and saturation, because the measurement scale differences between seismic data and log data and lab data make the relations not correct. Dvorkin and Uden (2006) studied the challenges in seismic-scale reservoir prediction on model data by Backus average method (Dvorkin and Uden, 2006; Backus, 1962). In our study, we also similarly analyzed the effects of scale on the time-lapse seismic study by Hashin-Strikman bounds theory (Berryman, 1995; Hashin and Shtrikman, 1963). The computed results are

shown as in Figure 5 and Figure 6. In seismic scale, the impedance differences caused by water saturation variation are dependent on the formation thicknesses. The impedance differences are not consistent with those in the accurate models.

Since it is difficult and complex to accurately compute the variation of each gas sand layer on the impedance data, we take all the single layers as a whole, and compute the accumulative P-wave and S-wave impedance differences of the whole gas formation. Besides the impedance variations, the computed accumulative P-wave and S-wave impedances differences of the gas formations are also affected by the varying formation thicknesses. So we compute the average accumulative P-wave and S-wave impedance differences by dividing them by the corresponding formation thicknesses. The accumulative difference attributes are mainly affected by the summation, that is, the quantity of the gas reservoir variations. While the accumulative difference attributes average mainly are affected by the change of a unit formation, that is, the quality of the gas reservoir variations. To quantitatively evaluate the real gas reservoir variations, we compute

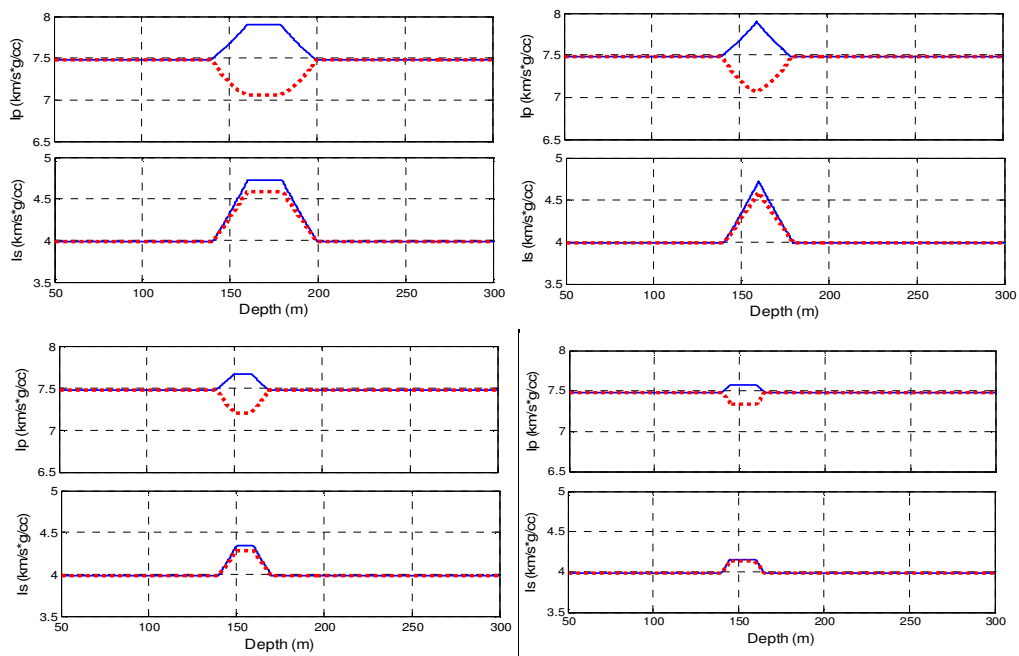


**Figure 6.** The seismic-scale models of P-wave impedance and S-wave impedance with different sand formation thicknesses computed from the models in Figure 5 by averaging the Hashin-Strikman bounds. Others are same as Figure 5.

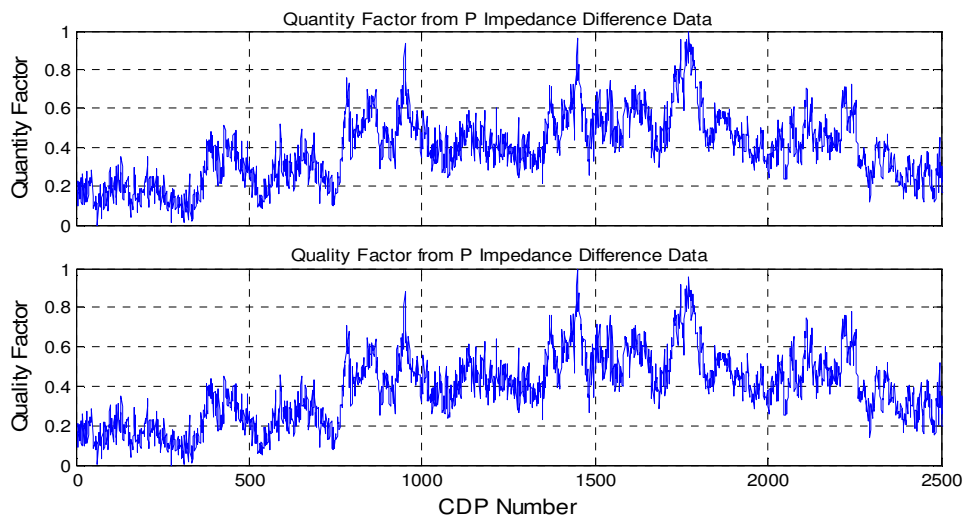


**Figure 7.** The quantity factor (top) and the quality factor (bottom) from P-wave impedance difference data versus CDP Number for the real gas reservoir.

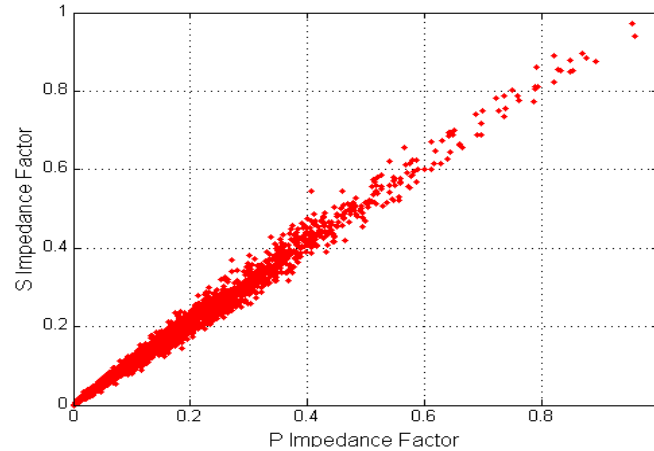


**Figure 8.** The cross-plot of the factor from P-wave impedance difference and the factor from S-wave impedance difference

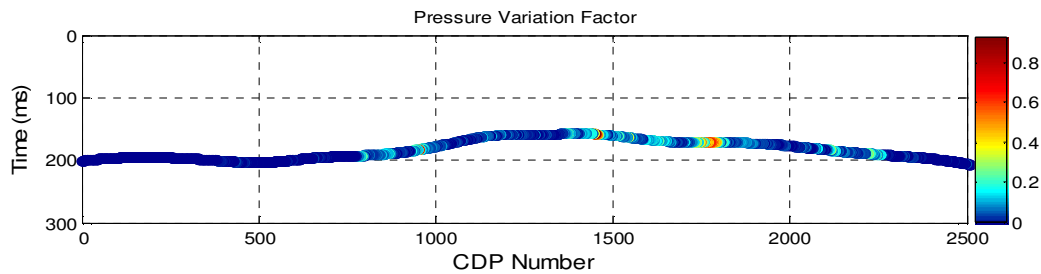


**Figure 9.** The relative variations of the effective pressure versus CDP number in the real gas reservoir. The color-bar is the factor of relative variations of the effective pressure

the quality factor ( $f_{Qual}$ ) and the quantity factor ( $f_{Quan}$ ) using equations (10) and (11) on the accumulative attributes and their averages.

$$f_{Qual} = \frac{D_{I\_Acc\_Ave} - Min\_D_{I\_Acc\_Ave}}{Max\_D_{I\_Acc\_Ave} - Min\_D_{I\_Acc\_Ave}} \quad (10)$$

$$f_{Quan} = \frac{D_{I\_Acc} - Min\_D_{I\_Acc}}{Max\_D_{I\_Acc} - Min\_D_{I\_Acc}} \quad (11)$$

Where,  $D_{I\_Acc}$  and  $D_{I\_Acc\_Ave}$  are the accumulative impedance difference attributes and their average attributes respectively.  $Max\_D_{I\_Acc\_Ave}$  and  $Min\_D_{I\_Acc\_Ave}$  are the maximum and minimum values of the accumulative impedance difference average attributes respectively.  $Max\_D_{I\_Acc}$  and  $Min\_D_{I\_Acc}$  are the maximum and minimum values of the accumulative impedance difference attributes respectively. For the P-wave impedance difference data of the real gas reservoir, the quality factor and the quantity factor versus CDP are shown as in Figure 7.

Figure 7 shows that the formation thicknesses variations cause little differences between the quality factor and the quantity factor. Since the rock physics study has shown that the variation of the effective pressure can cause both P-wave and S-wave impedance differences increase, we can take the products of the quality factors and the quantity factors from P-wave and S-wave impedance difference respectively as the factors of the real gas reservoir variations. And we also analyzed the gas reservoir variations by the cross-plot of these factors, shown as in Figure 8. The cross-plot shows that both P-wave and S-wave impedance differences increase at the same time. So the main reason cause the gas reservoir elastic parameters vary is the effective pressure, not the water saturation. This result is consistent with the fact that the bottom water is not active in the gas reservoir. We also take the products of the factor from P-wave impedance difference and the factor from S-wave impedance difference as the factor for quantitative analysis. The computed results provide us with the relative variations of the effective pressure in the real gas reservoir, shown

as in Figure 9.

## CONCLUSION

In the work, we study a pressure monitoring case in the real thin inter-layer gas reservoir by time-lapse seismic method. The time-lapse elastic impedance difference inversion method was presented and applied in the real gas reservoir, which used the pre-stack time-lapse seismic difference data and difference model, constructed on log data before and after reservoir development, as constraints to obtain P-wave and S-wave impedance differences directly. And, to obtain the elastic parameters variations in seismic scale, we computed the accumulative impedance differences and the average accumulative impedance differences of the real thin inter-layer gas reservoir. Then, we analyzed the relative variations of the effective pressure using cross-plot and the products of these factors from P-wave and S-wave impedance differences. The computed results have good conformance with the matters of fact of the real gas reservoir.

## ACKNOWLEDGEMENTS

I thank National Natural Science Function of China (No.41074098) and National 973 Basic Research Program (No.2007CB209606) for providing financial support to this study. I also thank the senior scientist Dr. Jack Dvorkin in Stanford University for his help and supervision during my study in SRB project.

## REFERENCE

Backus E (1962). Long-Wave Elastic Anisotropy Produced by Horizontal Layering, *Journal of Geophysical Research*. 67(11): 4427-4440

Batzle M., Wang Z (1992). Seismic properties of pore fluids: *Geophysics*. 57, 1396-1408.

Berryman JG. (1995). Mixture theories for the rock properties. In *Rock Physics and Phase Relations: A Handbook of Physical constants*, ed. T.J. Ahrens. Washington, DC: American Geophysical Union, 205-228

Brown S, Bussod G., Hagin, P (2007). AVO monitoring of CO<sub>2</sub> sequestration: a benchtop-modeling study, *The Leading Edge*. 26(12): 1576-1583

Connolly P (1999). Elastic Impedance: *The Leading Edge* 18: 438-452.

Davis TL, Benson R.D (2008). Pressure monitoring in tight gas exploration and production with multicomponent seismic data, *World Oil*. 229 (10).

Dvorkin J, Uden R (2006). The challenge of scale in seismic mapping of hydrate and solutions, *The Leading Edge*. 25(5): 637-642

Eberhart-Phillips D, Han D, Zoback D (1989). Empirical relationships among seismic velocity, effective pressure, porosity and clay content in sandstone: *Geophysics* 54, 82-89.

Gassmann F, (1951). Elasticity of porous media: Uber die elastizitat poroser medien: *Vierteljahrsschrift der Naturforschenden Gessellschaft*, 96, 1-23.

Greg A, Jack B, Kevin P (2000). Upscaling petrophysical propertied to the seismic scale, *SEG Annual Meeting*

Hashin Z, Shtrikman S, (1963). A variational approach to the theory of elastic behavior of multiphase materials. *J. Mech. Phys. Solids*. 11, 127-140

Landro M (2003). Discrimination between pressure and fluid saturation changes from marine multicomponent time-lapse seismic data: *Geophysics*. 66, 836-844.

Maffioletti F, Bardini S, Grana D (2010). Changing scale and domain of a petrophysical and elastic properties based log-facies classification, *SEG Annual Meeting*. 2406-2410

Mavko G., Mukerji T, Dvorkin J (2009). *The rock physics handbook*, Cambridge University Press.

Shapiro S (2003). Elastic piezosensitivity of porous and fractured rock; *Geophysics*. 68, 482-486.

Ying Z, Laurence R. (2003). Time-lapse well log analysis, fluid substitution and AVO. *The Leading Edge*. 22, 550-554.

Zeng H (2009). How thin is a thin bed? An alternative perspective, *The Leading Edge*. 28(10): 1192-1197